Trimethylaluminum Dimer Structure and Its Monomer Radical Cation: A Density Functional Study

Dorothée Berthomieu,*,† Yannick Bacquet,‡ Luca Pedocchi,‡ and Annick Goursot‡

LMPM, FOR 5635 CNRS, ENSCM, 8 rue de l'Ecole Normale, 34296 Montpellier Cédex-5, France, and UMR 5618 CNRS, ENSCM, 8 rue de l'Ecole Normale, 34296 Montpellier Cédex-5, France

Received: November 10, 1997; In Final Form: April 3, 1998

Molecular structures, energies, vibrational frequencies, and dissociation energies for $Al(CH_3)_3$, $Al(CH_3)_3^+$, and $[Al(CH_3)_3]_2$ have been studied using density functional and Møller−Plesset perturbation methods. The calculated properties are compared with the available experimental results. All the methods correctly describe the geometries of the neutral molecules. Density functional or MP2 (or MP4) methods provide similar ionization energies, whereas the dissociation energy of the dimer is more dependent on the methodology.

1. Introduction

The Lewis acid trimethylaluminum (TMA) is used in many catalytic processes and in organometallic chemistry. It is also used as an aluminum precursor for the preparation of thin solid films containing aluminum prepared by CVD (chemical vapor deposition) or PECVD (plasma-enhanced chemical vapor deposition) techniques.[1−6] When these techniques are used, different processes occur such as fragmentation and ionization, leading to various species. The knowledge of their energetics is thus important for a further study of the formation of the aluminum materials. Different experimental measurements, i.e., infrared and emission spectroscopy,[7,8] mass spectrometry,[8] and X-ray photoelectron spectroscopy,[3] have been devoted to the study of the TMA and of aluminum deposition mechanisms.

It was shown very early that, at room temperature, TMA has partly a dimer structure.[9] The structures of both TMA and its dimer TMA_2 have been determined by gas-phase electron diffraction,[10] whereas TMA2 has also been studied in the solid state by X-ray analysis.[11] These two methods lead to a dimer structure that contains two pentacoordinated carbon atoms, in contrast with a previous proposal, also based on X-ray diffraction data, that the ring system involves hydrogen-bridged bonds[12,13] (Chart 1).

Both the gas-phase and solid-state studies assume explicitly that the AlCAlC ring is planar.[10,11] The dissociation energy of TMA: has been evaluated at 20.2 ± 1.0 kcal/mol from a vapor pressure measurement,[9] which characterizes a substantial binding between two TMA moities including two pentavalent carbons.

We have found it interesting to explore the potential energy surface of the TMA dimer with different methodologies, i.e., DFT, HF, and post-Hartree−Fock, comparing their description of the TMA_2 electronic structure. We have been interested in predicting the first ionization energy of this compound. Its eventual difference with the first ionization energy of TMA could indicate the possible separation of TMA and TMA_2 through ionization processes. The geometry and ionization energy of the monomer have been studied providing a reference for TMA_2. Finally, the vibrational analyses of TMA and TMA_2 have been performed and compared with the experimental spectra.

CHART 1

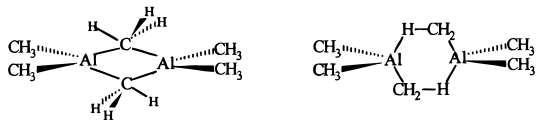

2. Computational Methods

Ab initio calculations have been performed using the Gaussian94 package.[14] The electron correlation energy is then introduced using the MP2 (second-order Møller−Plesset)[15] or MP4 (fourth-order Møller−Plesset) approach with single, double, triple, and quadruple subtitutions.[16,17] In the case of the monomer, we have also used the coupled-cluster singles and doubles approach,[18−20] using a perturbational estimate of the contribution of the triple excitations.[21] This method is denoted CCSD(T). Density functional calculations have been performed with the Gaussian94 package and the deMon code.[22] Gradient-corrected functionals have been used for the exchange−correlation potential and energy, namely, the Becke exchange[23] and Perdew correlation[24] functionals (BP86) and the Perdew and Wang exchange and correlation functionals (PW91).[25] The nonlocal Becke exchange[23] and Perdew and Wang correlation functional[25] (BPW91) have also been used with the Gaussian94 program.

The geometries have been fully optimized without any assumption (except for the calculation of the vertical ionization energy). The Gaussian basis set 6-31G(d,p) has been used for the Hartree−Fock, post-Hartree−Fock, and DF calculations using the Gaussian94 package. The notations HF, MP2, $BP86_G$, and $BPW91_G$ are used for these calculations, respectively. The notations MP4(SDTQ)//MP2 and CCSD(T)//MP2 are used for MP4(SDTQ) and CCSD(T) calculations, respectively, at the MP2 optimized geometries.

For the calculations using the deMon code, the orbital bases are (41/1) for H, (5211/411/1) for C, and (6321/521/1*) for Al.[26] The corresponding auxiliary basis sets are (5,1;5,1) for H,

* Corresponding author.
† LMPM, UMR 5635 CNRS.
‡ UMR 5618 CNRS.

S1089-5639(98)00148-0 CCC: $15.00
Published on Web 08/19/1998

TABLE 1: Calculated and Experimental Geometrical Parameters of $Al(CH_3)_3$. Bond Lengths in Angstroms, Valences Angles in Degree,[a] Standard Errors

		Al_1-C_1	Al_1-C_2	Al_1-C_3	C−H	$C_1Al_1C_2$	$C_1Al_1C_3$
HF	TMA	1.98	1.98	1.98	1.08	120.0	120.0
MP2	TMA_a	1.97	1.97	1.97	1.09	120.0	120.0
BP86G	TMA_a	1.98	1.98	1.98	1.10	119.98	119.95
BP86	TMA_a	1.97	1.97	1.97	1.11	119.90	119.90
	TMA_b	1.97	1.97	1.97	1.11	119.97	119.93
experiment[10]	TMA	1.957(3)[a]	1.957(3)	1.957(3)	1.113(3)	$120_{assumed}$	
$D_{3h}(AlC_3$ trunk)							

(5,2;5,2) for C, and (5,4;5,4) for Al. The basis set 6-31G(d,p) would correspond to (31/1) for H, (631/31/1) for C, and (6631/631/1) for Al.

Bond orders, which are used to compare bonding properties, have been calculated according to Mayers's definition.[27] The DFT approach deals with the electronic density of a system, but Kohn−Sham orbitals can always be used, as well as Hartree−Fock orbitals, in order to build a Slater determinant, which constitutes the approximate ground-state wave function. Bond orders, calculated from this wave function, are very useful quantities that allow discussion of chemical properties.

Vibrational analyses have been performed to ensure that the optimized geometries correspond to minima on the PES (potential energy surface). Hartree−Fock and Gaussian94-DF frequencies are calculated using analytical second derivatives, whereas MP2 and deMon-DF results are obtained from the evaluation of numerical second derivatives.

The BSSE correction (basis set superposition error) has been evaluated as less than 0.1 kcal/mol for the weaker dimer. For the other dimer complex, the TMA subunit is so different from the geometry of an isolated TMA that it has not been possible to evaluate the BSSE, using the most widely used counterpoise procedure.[28]

Finally, unrestricted Hartree−Fock and Kohn−Sham wave functions have been used for open shell systems. $\langle S^2 \rangle$ values have been evaluated from these wave functions.

3. Results and Discussions

A. Equilibrium Geometries of TMA, TMA^+, and TMA_2. According to gas-phase electron diffraction data,[10] the monomer TMA has D_{3h} symmetry with freely rotating methyl groups. DF calculations yield two stable rotational isomers TMA_a and TMA_b and one transition state TMA_c. From Table 1, one can see that, even though no symmetry has been imposed, the conformer TMA_a has, taking into account computational errors, a C_{3h} symmetry (Figure 1). Due to the planarity of the molecule and to the large Al−C bond lengths, we can expect that the steric hindrance is small and the smallest one does indeed correspond to this conformer. The isomer TMA_b has a C_s-like geometry and is 0.1 kcal/mol less stable than TMA_a. The structure TMA_c, which possesses an imaginary frequency, has a C_{3v}-like geometry, if one includes the hydrogen atoms, and its energy difference with TMA_a amounts also to only 0.1 kcal/mol. At this level of theory, one can thus consider that the potential energy surface is very flat, leading to a free rotation of the methyl groups, as proposed from experiments in the gas phase and from previous OF calculations.[10,29] As shown in Table 1, the geometries obtained with the different methods are very comparable. The isomer TMA_a has been chosen to calculate the energetics and spectroscopic properties.

The highest molecular orbital (HOMO) of TMA_a has an E′ symmetry involving the p_xp_y orbitals of the aluminum atom and is fully occupied. As expected, the removal of an electron leads to a Jahn−Teller distortion for TMA^+ when its structure is

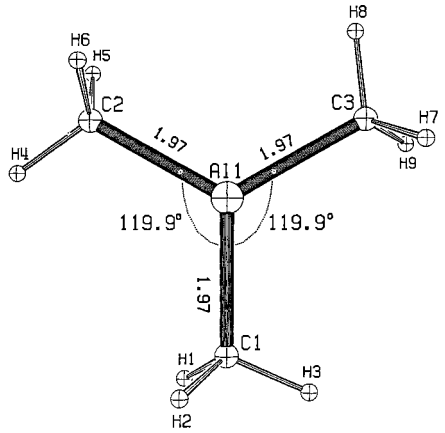

Figure 1. Calculated BP86 $Al(CH_3)_3(TMA_a)$ structure. Bond lengths in angstroms.

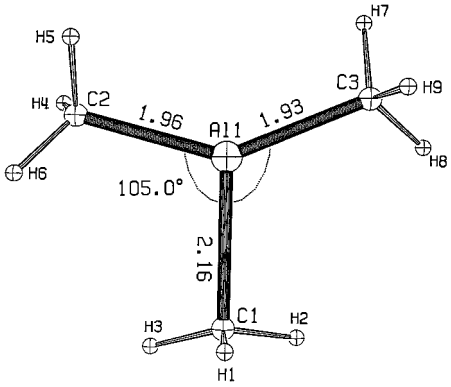

Figure 2. Calculated BP86 $Al(CH_3)_3^+(TMA_\alpha^+)$ structure. Bond lengths in angstroms.

allowed to relax: starting from TMA_a the two ionic structures TMA^+_α (Figure 2) and TMA^+_β have been obtained after geometry optimization (Table 2). We have verified that these two minima are really separated structures although their energy difference is only 0.4 kcal/mol. Despite their similar energies, these structures, which possess a quasi-C_s symmetry, are significantly different. Each species has modified valence angles with respect to the neutral TMA: with one (TMA^+_α) or two (TMA^+_β) substantially increased CAlC angles (Table 2) (141.9° (TMA^+_α) or 128.4° (TMA^+_β) (Table 2)). Moreover, TMA^+_α has one bond length increased with respect to the neutral form, whereas TMA^+_β has two elongated Al−C bonds (Table 2).

The Mayer bond order analysis confirms that one bond is weakened in TMA^+_α, against two for TMA^+_β, with calculated bond orders of 0.60, 1.07, and 0.99 for the three Al−C bonds in TMA^+_α and of 0.82, 1.11, and 0.76 in TMA^+_β. The unimolecular dissociation of an ionized TMA has been reported from a mass spectrometry experiment.[30] The base peak, i.e. the most abundant, corresponds to the unimolecular dissociation of the molecular ion, leading to $Al(CH_3)_2^+$. The dissociation of TMA^+_α into $Al(CH_3)_2^+$ and a methyl radical corresponds to

TABLE 2: Relaxed structures of the $Al(CH_3)_3^+$ Ion. Bond Lengths in Angstroms and Valence Angles in Degrees

		Al_1-C_1	Al_1-C_2	Al_1-C_3	C−H	$C_1Al_1C_2$	$C_2Al_1C_3$
HF	TMA^+_α	2.45	1.94	1.94	1.08	102.6	154.6
MP2	TMA^+_α	2.38	1.93	1.93	1.08	103.2	153.5
$BP86_G$	TMA^+_α	2.22	1.96	1.96	1.10	107.5	144.9
	TMA^+_β	2.05	1.93	2.08	1.10	134.2	128.4
BP86	TMA^+_α	2.16	1.96	1.93	1.11	105.0	141.9
	TMA^+_β	2.04	1.92	2.05	1.11	133.4	128.2

TABLE 3: Geometrical Parameters of the Dimer $[Al(CH_3)_3]_2$ (Bond Lengths in Angstroms and Angles in Degrees)

	Al_1-C_{1br}	Al_1-C_5	$Al_1\cdots Al_2$	$C_5\cdots C_6$	$Al_1-C_{2br}-Al_2$	$C_{2br}-Al_1-C_{1br}$	$Al_1-C_{2br}-Al_2-C_{1br}$
isomer A BP86	3.94	1.97	5.02	3.41	109.9	70.9	0.0
isomer A HF	4.07	1.98	5.10	3.42	109.9	70.9	0.0
isomer B BP86	2.16	1.96	2.63	3.44	74.8	104.0	11.4
isomer B HF	2.16	1.98	2.63	3.46	74.9	104.0	11.1
isomer B PW91	2.10	1.92	2.56	3.41	75.1	102.0	18.3
isomer B MP2	2.15	1.97	2.60	3.47	74.7	101.1	11.8
isomer B $BP86_G$	2.17	1.98	2.62	3.47	74.3	104.3	12.8
isomer B $BPW91_G$	2.17	1.98	2.62	3.46	74.2	104.4	12.6
exp[10] D_{2h}	2.140(4)[a]	1.957(3)	2.619(5)	3.344(28)	75.5(0.1)	104.5(0.1)	$0_{assumed}$
exp[11] C_{2h}[b]	2.125(2)	1.956(2)	2.606(2)		75.7(1)	104.3(1)	$0_{assumed}$

[a] Standard errors. [b] The primary deviation from C_{2h} was only a slight shift of a H−C bridge out of the mirror plane by 3.3 ± 2.2°.[11]

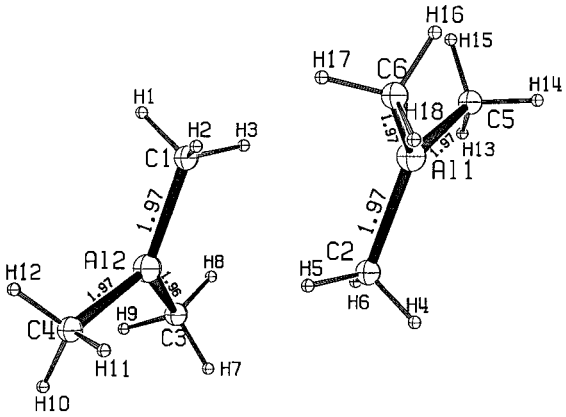

Figure 3. Calculated BP86 $[Al(CH_3)_3]_2$ structure, isomer A. Bond lengths in angstroms.

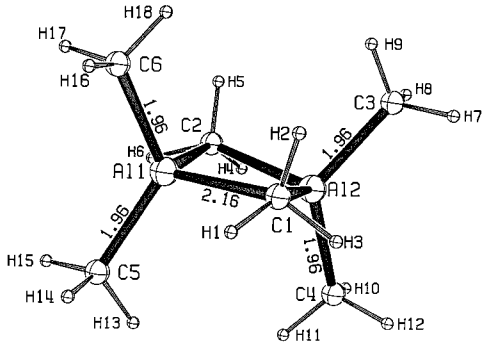

Figure 4. Calculated BP86 $[Al(CH_3)_3]_2$ structure, isomer B. Bond lengths in angstroms.

an endothermic reaction with a calculated dissociation energy of 22.6 kcal/mol using BP86 and 24.3 kcal/mol using the PW91 functionals (without taking into account ZPE and BSSE corrections). A previous semiempirical calculation also concluded an endothermic dissociation of only 7 kcal/mol.[31] From experiment, the dissociation energy is evaluated at 27 kcal/mol.[30,32] We failed to find a transition state for the dissociation involving the longest A1−C bond, suggesting that the fragmentation occurs after ionization through a straighforward process.

Like many compounds including IIIA elements, TMA, at room temperature, is in equilibrium with TMA_2.[9] In the gas phase, TMA_2 has been reported as characterized by a ring system involving two aluminum and two carbon atoms, the planarity of this system being assumed.[10,11] Moreover, another solid-state experiment concludes some deviation from D_{2h} symmetry of the skeleton.[13]

A previous theoretical investigation of TMA_2[33] found a weak complex with C_{2h} symmetry in disagreement with the gas-phase electron and X-ray diffraction determination. In fact, our study has led to two stable structures A and B. which are presented in Table 3.

The species A (Figure 3) involves a nonconstrained ring $[Al_1C_1Al_2C_2]$ and is very similar to the loose C_{2h} structure calculated by Hiraoka et al.,[33] although the distance we obtain between the two TMA subunits is longer ($Al_1\cdots Al_2$ is 5.10 Å instead of 4.44 Å and $Al_1\cdots C_{1bridge}$ is 4.07 Å instead of 3.60 Å). The four-ring system of this structure is planar, and each TMA retains its isolated geometry (Al−C bond lengths of 1.97A).

The second minimum localized on the PES (structure B) is displayed in Figure 4. The geometries of this isomer obtained with the different theoretical methods are very comparable, although the structure obtained with the PW91 functionals leads to a somewhat more compact structure. Two other methyl rotational isomers B′ and B″ have also been found (MP2 calculations). Whereas isomer B has two eclipsed bridging CH_3 groups, they are staggered in isomer B′. The terminal CH_3 groups are eclipsed in isomer B and staggered in isomer B″, B″ being less stable than B (less than 2 kcal/mol). Isomers B and B′ have comparable energies, B being more stable than B′ by only 0.3 kcal/mol, which suggests that the H atoms of the C_{bridge} do not contribute to the stabilization of the dimer. As shown in Figure 4, the isomer B has a C_{2v}-like geometry. Its bridging CH_3 groups do not contain hydrogen atoms in the Al−C−Al planes, which indicates that there are no stabilizing Al···H bonds. Even in the weak complex A, we could not obtain a stable compound with a methyl group directing one H atom toward the Al of the second moiety. These conclusions are confirmed by the Mayer bond order analysis (Table 4), which indicates that the $Al-C_{bridge}$ bonds are twice as weak as the

TABLE 4: Bond Order Analysis of TMA and Its Dimer (BP86 Calculation)

bond	$Al(CH_3)_3$ TMA_a	bond	$[Al(CH_3)_3]_2$ isomer B
Al_1-C_1	0.98	Al_1-C_1	0.52
Al_1-C_2	0.97	Al_1-C_2	0.52
Al_1-C_3	0.97	Al_1-C_5	1.00
		Al_1-C_6	1.03
		Al_1-H_1	0.06
		Al_1-H_2	0.02
Al_1-H_3		Al_1-H_3	0.02
C_1-H_1	0.98	C_1-H_1	0.90
C_1-H_2	0.98	C_1-H_2	0.99
C_1-H_3	0.98	C_1-H_3	0.90

four other Al−C bonds and that the hydrogen atoms of the bridging methyl groups do not participate in the TMA−TMA bonding since the $Al\cdots HC_{bridge}$ bond orders are very small. If a C_{2h}-like geometry is imposed by rotating the bridging methyl groups, the energy is raised by 20 kcal/mol ($BP86_G$ calculation). A subsequent optimization leads back to the isomer B with C_{2v}-like geometry. This result also suggests that there is no free rotation of the methyl bridge groups.

Two carbon atoms (C_1 and C_2, labelled as C_{bridge}, in Table 3) and two aluminum atoms are involved in the four-membered ring. The bonds and angles of the TMA subunits are very different from those of the isolated TMA, and the dimer does not look like a van der Waals complex but more like a covalent structure. Each monomer contains two increased $Al-C_{bridge}$ bonds involved in the $[Al_1C_1Al_2C_2]$ ring. While the isolated TMA is planar, it becomes pyramidal when involved in the complex. The four-membered ring system $[Al_1C_1Al_2C_2]$ is very constrained and resembles a rhombus with one atom sligthly outsides the plane (0.42 Å with BP86). If a planar ring is imposed, the energy of the system increases. This result shows that the planarity of the ring induces a constraint which is relaxed in the nonplanar structure. In contrast, the two planes, each one involving an aluminum atom and its two terminal carbon atoms, are parallel ($C_5C_6Al_1$ and $C_3C_4Al_2$) (Figure 4), whereas a distortion is reported from a solid-state experiment.[13]

As shown in Table 3, the geometry of structure B is very close to the gas-phase electron diffraction[10] and X-ray diffraction[11] experimental results. The differences in bond lengths and bond angles are within both the experimental and numerical error bars. However, these calculations show that a rearrangement from C_{2h} symmetry through small adjustments of dihedral angles provides a substantial stabilization and leads to a more stable C_{2v}-like geometry.

B. Ionization and Binding Energies. If the first ionization energy of TMA has been measured, there is, to our knowledge, no experimental value available for the dimer. Moreover, the two values presented in the literature for the monomer are quite different, i.e., $9.0_9 \pm 0.2_6$ eV and <9.76 eV.[30,34]

We have calculated vertical and adiabatic ionization energies for TMA using various levels of theory (Table 5). The different levels of correlation do not modify very significantly the values, with a tendency of some overestimation by the MP2 with respect to MP4 Møller−Plesset and CCSD(T) methods. An overestimated ionization energy value is also calculated using a smaller basis set. With the same basis set, the density functional calculation $BP86_G$ leads to IE values very similar to MP2. The comparison between $BP86_G$ using two different basis set extensions and BP86 values shows that the numerical uncertainty, which includes errors due to grid calculations and SCF convergence, is not negligible, since it reaches here 0.22 eV (Table 5).

The vertical ionization energy of the dimer B, which corresponds to the most stable minimum, has also been evaluated using the different methods and basis set extensions (Table 6). The HOMO of TMA_2 involves essentially p orbitals of the aluminum and terminal carbon atoms. In fact, the HOMO and the molecular orbital just below it are almost degenerate and represent the components of a local E symmetry. The removal of one electron from the HOMO leads to different vertical IE values according to different methods. Indeed, the calculated $BP86_G$ and MP2 vertical IEs differ by 0.81 eV (Table 6). The analysis of the corresponding TMA_2^+ orbitals shows that this difference originates from a difference in the final electronic state. In fact, on one hand (BP86, PW91, $BP86_G$), the hole is delocalized equally on the two $Al(CH_3)_2$ groups, whereas, on the other hand (HF, MP2), the hole is localized on only one $Al(CH_3)_2$ group, i.e., on one subunit of the complex. In both cases, the electrons of the CH_3 bridging groups are not concerned. The lowest vertical IE obtained for the delocalized hole suggests that this ionic configuration is the most stable. Numerical effects between programs are less than 0.2 eV, which corresponds to the value obtained for the monomer (BP86, $BP86_G$). The ionic species obtained with MP2 can also be obtained with a DF method, constraining the hole to be localized on one TMA subunit. The corresponding ionization energy (BP86) is then increased by 0.78 eV. These results show that the IE of the dimer is lower than that of the monomer, by about 1 eV, which indicates that TMA^+ and TMA_2^+ could be separated by ionization techniques. In both open shell systems, TMA^+ and TMA_2^+, $\langle S^2 \rangle$ is very close to 0.75, which confirms

TABLE 5: Vertical and Adiabatic Ionization Energy of $Al(CH_3)_3$ in eV

	vertical IE	adiabatic IE (with ZPE)
HF	9.00	7.76 (7.73)
	$\langle S^2 \rangle = 0.77$	$\langle S^2 \rangle = 0.76$
MP2	9.67	8.63 (8.60)
	$\langle S^2 \rangle = 0.77$	$\langle S^2 \rangle = 0.76$
MP4(SDTQ)//MP2	9.62	8.62
	$\langle S^2 \rangle = 0.77$	$\langle S^2 \rangle = 0.76$
CCSD(T)//MP2	9.53	8.60
	$\langle S^2 \rangle = 0.77$	$\langle S^2 \rangle = 0.75$
$BP86_G$	9.68	8.65 (8.61)
	9.45[a]	8.83[a]
	$\langle S^2 \rangle = 0.75$	$\langle S^2 \rangle = 0.75$
BP86	9.23	8.83
	$\langle S^2 \rangle = 0.75$	$\langle S^2 \rangle = 0.75$
experiment[30,34]	$9.0_9 + 0.2_6$ and <9.76	

[a] IE using the basis set of BP86 calculation.

TABLE 6: Dissociation Energy of the Dimer $[Al(CH_3)_3]_2$ in kcal/mol with Respect to TMA_a and Vertical Ionization Energy of the Dimer $[Al(CH_3)_3]_2$ (Isomer B) in eV

	dissociation energy		vertical IE
	TMA_2 isomer A (with ZPE)	TMA_2 isomer B (with ZPE)	TMA_2 isomer B
$HF_{[33]}$	(1.2)		
HF	1.0 (0.5)	4.5 (1.9)	8.95
			$\langle S^2 \rangle = 0.77$
$BP86_G$		15.5	8.77(8.75)[a]
			$\langle S^2 \rangle = 0.75$
$BPW91_G$		14.4	8.31
			$\langle S^2 \rangle = 0.75$
MP2		20.0 (17.4)	9.58
			$\langle S^2 \rangle = 0.77$
BP86	0.4	11.6 (9.0)	8.63
			$\langle S^2 \rangle = 0.75$
PW91		15.3	8.62
			$\langle S^2 \rangle = 0.75$

[a] Vertical IE using the geometry and basis set of BP86 calculation.

TABLE 7: Observed and Calculated Infrared Spectra (cm^{-1}) of Monomeric Trimethylaluminium TMA_a[a]

ν_{obs}[b]	assignment of mode[b]	ν_{calc}[c]	intensity$_{calc}$[c]	assignment of mode[c]
		19	0	bending twisting CH_3
		31	0	bending twisting CH_3
		51	0	bending twisting CH_3
		165	2.3	scissoring AlC
		167	2.4	scissoring AlC
		178	3.7	wagging AlC
		498	0	s-stretching AlC
		551	0	twisting CH_3
		555	0	twisting CH_3
		583	0	twisting CH_3
		626	11	stretching AlC, twisting CH_3
		627	10	s-stretching AlC, twisting CH_3
691 m,sh	a-stretching CH	719	108.9	twisting CH_3
744 vs	rocking CH_3	755	161.8	stretching AlC wagging CH_3
754 s,sh	rocking CH_3	756	161.6	stretching AlC wagging CH_3
1202 s	s-bending CH_3	1208	28.7	a-stretching AlC bending CH_3
		1209	27.0	s-stretching AlC bending CH_3
		1214	1.7	s-stretching AlC bending CH_3
		1421	0.5	scissoring CH_3
		1422	0.5	scissoring CH_3
		1423	0	twisting CH_3
		1423	0	twisting CH_3
		1424	0	twisting CH_3
1430 ww	a-bending CH_3	1427	3	twisting CH_3
		2951	9.5	s-stretching CH
2901 m	s-stretching CH	2952	9.7	s-stretching CH
		2954	0.5	s-stretching CH
		3020	13.6	a-stretching CH
		3021	13.4	a-stretching CH
		3022	18.4	a-stretching CH
		3049	9.9	stretching CH
2982 m	a-stretching CH	3050	26.3	stretching CH
		3052	21.5	stretching CH

[a] Abbreviations: s = strong, m = medium, w = weak, v = very, sh = shoulder. [b] From ref 29. [c] From $BP86_G$.

that the spin contamination is negligible (Tables 5 and 6). As already reported,[35,36] DFT solutions are less contaminated by higher spin states than their UHF counterparts.

The interaction energy between the two TMA moieties is also reported in Table 6. The small interaction energy (less than 1.0 kcal/mol) calculated for the isomer A shows that it is a van der Waals complex. One can thus expect that, at room temperature, this complex decomposes easily.

The diversity of the calculated interaction energy values for the isomer B suggests that the dimer electronic structure is very sensitive to correlation effects. To evaluate the effects due to the basis extension and to the approximations of the methods, DF calculations have been performed using both the same 6-31G(d,p) basis ($BP86_G$ and $BPW91_G$) as for MP2 and the more extended basis as described in the computational method (BP86, PW91). As one can see from Table 6, these interaction energies display differences comparable with those induced by the choice of the functionals. These results show that both basis set extension and the choice of the approximate exchange and correlation functionals are critical factors for the study of intermolecular interactions. The MP2 value obtained with the 6-31G(d,p) basis is close to the experimental result, which is 20.2 ± 1.0 kcal/mol.[9] However this agreement may be fortuitous since MP2 calculations may overestimate correlation energy. With ZPE corrections, the calculated enthalpy of dissociation ranges between 9 and 17 kcal/mol (Table 6).

C. Vibrational Frequencies of TMA and TMA_2. The vibrational frequencies of TMA and TMA_2 have been evaluated using the harmonic approximation, with both HF and DFT approaches. Previous HF calculations were already reported for TMA[29,37] and for the loose structure of TMA_2.[33] However, they were based, for TMA, on a HF calculation using a very small basis set and, for the dimer, on calculations using the Wilson's GF matrix method.[38] Moreover, there was no previous quantum chemical calculation for the stable structure B. The comparison of our HF and DFT frequencies with the experimental IR spectra of TMA and TMA_2 shows that the DFT calculations are the most reliable ones to interpret these spectra. Our calculated spectrum for the isomer A of TMA_2 is comparable with that published by Hiraoka. However, its comparison with the experimental spectrum shows that this isomer does not correspond to the real dimer. Indeed, there is no signal in the far infrared spectrum of structure A, whereas there is one intense band in the 200−500 nm region spectrum of TMA_2. In contrast, the calculated vibrations for the structure B of TMA_2 are in good agreement with the experimental spectrum. The DFT spectra ($BP86_G$) of TMA and TMA_2 are compared with the experimental ones in Table 7 and Table 8, respectively.

For TMA, our assignments differ generally from those proposed previously.[29] Indeed, these previous assignments interpret the bands as characteristics of a single group, whereas our normal mode analysis shows that they correspond most generally to a combination of the vibrations of several parts of the system. The calculated IR spectrum of TMA in vapor state is characterized by very strong peaks in the low-energy region (Table 7). According to our calculation, the experimental peak at 691 cm^{-1} corresponds to a CH_3 twisting and those at 744 and 754 cm^{-1} to Al−C stretching mixed with CH_3 wagging. The peak at 1430 cm^{-1} corresponds to the CH_3 twisting. The calculated frequencies are always slightly overestimated except in the region around 1430 cm^{-1}. Anharmonic corrections would decrease the frequencies by 30−50 cm^{-1}.

Concerning the TMA_2 complex, the calculated vibrational

TABLE 8: Observed and Calculated Infrared Spectra (cm^{-1}) of Dimeric Trimethylaluminum TMA_2 (Isomer B)[a]

ν_{obs}[b]	assignment of mode[b]	ν_{calc}[c]	intensity$_{calc}$[c]	assigment of mode[c]
		60	1.0	bending rocking AlC and twisting AlC_{bridge}
		89	0	bending twisting CH_3
		93	0	bending twisting CH_3
		97	0	twisting CH_3
		111	0	twisting CH_3
		113	0	bending twisting $C_{bridge}H_3$
		138	4.2	bending twisting $C_{bridge}H_3$
		140	0	scissoring AlC
		147	2.5	scissoring AlC_{bridge}
		157	0	twisting $C_{bridge}H_3$
		158	0	twisting $C_{bridge}H_3$
		161	3.7	scissoring AlC
		168	2.7	scissoring AlC
		170	0.6	twisting $AC_{bridge}H_3$
		194	1.3	scissoring twisting AlC
		294	0	bending rocking and a-stretching AlC_{bridge}
		308	0	bending scissoring AlC
368 s	stretching AlC_{bridge}	342	50.5	scissoring and s-stretching AlC_{bridge}
		434	0.2	s-stretchinging in the plane AlC_{bridge}
480 m	stretching AlC_{bridge}	474	48.0	a-stretching AlC
567 s	stretching AlC	546	96.6	s-stretching AlC
		558	0	bending twisting $C_{bridge}H_3$
		578	0.6	s-stretching AlC_{bridge}
		581	60.2	bending wagging CH_3
		591	0.3	bending wagging CH_3
		600	0.3	twisting CH_3
609 m	rocking CH_3	608	101.8	twisting $C_{bridge}H_3$ and wagging CH_3
		626	0	stretching AlC, CH_3, and $C_{bridge}H_3$ twisting
		630	15.8	a-stretching CH
650 vw	rocking CH_3	679	24.1	a-stretching CH
		691	11.8	wagging $C_{bridge}H_3$ and CH_3
		718	0	twisting CH_3
700 vs	stretching AlC	722	224.5	wagging CH_3
		725	212.7	twisting $C_{bridge}H_3$ and CH_3
		744	1.7	wagging CH_3
774 s	rocking $C_{bridge}H_3$	778	200.2	wagging $C_{bridge}H_3$ and CH_3
		1212	3.9	wagging CH_3 and stretching AlC
1208 s	s-deformation CH_3	1213	27.0	wagging $C_{bridge}H_3$ and CH_3 and stretching AlC
		1217	16.3	wagging CH and stretching AlC
		1223	30.8	wagging $C_{bridge}H_3$ and CH_3 and stretching AlC
1255 m	s-deformation $C_{bridge}H_3$	1248	43.0	wagging $C_{bridge}H_3$
		1253	0	wagging $C_{bridge}H_3$ and CH_3
		1411	0 .	twisting $C_{bridge}H_3$
		1414	0.0	scissoring and twisting $C_{bridge}H_3$
		1414	1.6	scissoring CH_3
		1415	1.3	scissoring CH_3 and $C_{bridge}H_3$
		1419	0	twisting CH_3
		1422	0.1	scissoring CH_3 and twisting $C_{bridge}H_3$
		1422	0	twisting CH_3 and $C_{bridge}H_3$
		1426	0.4	scissoring CH_3 and $C_{bridge}H_3$
		1431	1.7	scissoring CH_3
		1432	0	twisting CH_3
		1436	3.0	scissoring $C_{bridge}H_3$
		1438	4.3	twisting CH_3
		2935	2.1	s-stretching $C_{bridge}H$
		2936	0.6	a-stretching $C_{bridge}H$
		2953	3.6	a-stretching $C_{bridge}H$
		2953	17.9	s-stretching $C_{bridge}H$
		2955	15.4	s-stretching CH
		2955	3.5	s-stretching CH
2845 w	deformation	2983	0	$C_{bridge}H$ s-stretching
2904 m	s-stretching CH	2985	41.3	$C_{bridge}H$ s-stretching
2944 s	a-stretching CH_3	3026	0.0	s-stretching CH
3008 vw	stretching CH	3026	28.2	a-stretching CH
		3031	0.0	s-stretching CH
		3031	45.3	a-stretching CH
		3038	30.1	stretching CH
		3039	34.0	stretching CH
		3039	5.7	stretching CH
		3040	13.1	stretching CH
		3058	0.6	stretching $C_{bridge}H$
		3059	15.0	stretching $C_{bridge}H$

[a] Abbreviations: s = strong, m = medium, w = weak, v = very, sh = shoulder. [b] From ref 39. [c] From $BP86_G$.

frequencies are also in good agreement with experiment in the gas phase, although generally underestimated for low-frequency vibrations. This result is consistent with an underestimated TMA−TMA binding energy, since, in this region, the bands correspond to the vibrations of the skeleton.[39] Both the theoretical and experimental spectra of the dimer show medium and strong vibrations in the far IR region under 600 cm^{-1} which are not observed in the monomer spectrum. Strong skeletal vibrations are calculated at 342 cm^{-1} (368 cm^{-1} from experiment). This normal mode corresponds also to the scissoring of the AlC_{bridge}. The band at 474 cm^{-1} of medium intensity is assigned to the stretching mode of the terminal Al−C bonds. The very intense bands at 722 and 725 cm^{-1} (700 cm^{-1} from experiment) involve only bending modes of the $C_{bridge}H_3$ and CH_3 groups. We have attributed the other experimental intense band at 1208 cm^{-1} to the wagging mode of the $C_{bridge}H_3$ and CH_3 groups and to the streching Al−C vibrations. From our theoretical calculations, the strong vibration at 778 cm^{-1} corresponds to the waging $C_{bridge}H_3$ and CH_3 modes. Most generally, one can say that bridged and terminal methyl groups are involved together in the vibrations of large intensity.

4. Conclusion

A quantum chemical study of the TMA molecule, of its radical, cation and of its dimer has been performed using different levels of theory, HF, MP2, and DF calculations. Equilibrium geometries, ionization and binding energies, harmonic vibrational frequencies, and infrared intensities have been calculated for these molecules. The results obtained show that equilibrium geometries are in general good agreement with the available experimental data, whatever the method used. However, no calculation leads to a planar four-membered ring system $Al_1C_lAl_2C_2$ in the dimer TMA_2: a small deviation from planarity is always calculated. The interpretation of the X-ray diffraction data supposes a center of inversion to be present in the middle of the AlCAlC ring, which makes it inevitabley planar. Since the quality of the X-ray diffraction data (although apparently excellent) is not sufficient to detect the presence or absence of an inversion center, we may expect that TMA_2 has a C_{2v}-like symmetry instead of a C_{2h} symmetry.

The ionization energies and the dissociation energy are much more sensitive to the computational methodology. The uncertainty concerning IE values obtained with the different methods is 0.7 eV for the monomer. It is roughly the order of magnitude of the experimental error for the TMA molecule. Vertical ionization leads to a point on the ion potential energy surface that is not the minimum This can explain why different numerical techniques may generate different electron configurations and thus different ionization energies in the case of the dimer. One can consider that the IE of the dimer is smaller than that of the monomer, which may allow the separation of these two species by ionization processes. Because of computational errors, the determination of a valid dissociation energy for the TMA_2 system necessitates very sophisticated calculations. This property is very sensitive to the basis set extension and also to the description of the electronic correlation.

Finally, the calculated vibrations of TMA and TMA_2 are in good agreement with the experimental spectra. For TMA_2, the bands observed in the 300−600 cm^{-1} region are assigned to the vibrations of the AlCAlC ring, characteristic of the isomer B structure.

Acknowledgment. These calculations have been performed on the IBM SP2 computer of the CNUSC Center in Montpellier (Centre National Universitaire Sud de Calcul) and on the Cray C98 of the IDRIS Center (Institut des Ressources en Informatique Scientifique) in Orsay (France). We acknowledge Dr. Arie van der Lee for helpful discussions.

References and Notes

(1) Morita, M.; Uesugi, N.; Isogai, S.; Tsubouchi, K.; Mikoshiba, N. *Jpn. J. Appl. Phys.* **1981**, *20*, 17−23.
(2) Kawakami, H.; K. Sakurai, K.; Tsubouchi; Mikoshiba, N. *Jpn. J. Appl. Phys.* **1988**, *27*, L161−l163.
(3) Liu, H.; Bertholet, J. W.; Rogers, J. W. *Surf. Sci.* **1995**, *340*, 88−100.
(4) David, M.; Babu, S. V.; Rasmussen, D. H. *J. AIChE* **1990**, *36*, 871−876.
(5) Hasegawa, F.; Takahashi, T.; Kubo, K.; Ohnari, S.; Nannichi, Y.; Arai, T. *Jpn. J. Appl. Phys.* **1987**, *26*, L1448.
(6) Meikle, S.; Nomura, H.; Nakanishi, Y.; Hatanaka, Y. *J. Appl. Phys.* **1990**, *67*, 483−486.
(7) Soto, C.; Wu, R.; Bennett, D. W.; Tysoe, W. T. *Chem. Mater.* **1994**, *6*, 1705−1711.
(8) Bacquet, Y. Thesis, Université Montpellier II, 1997.
(9) Laubengayer, A.W.; Gilliam, W. F. *J. Am. Chem. Soc.* **1941**, *63*, 477−479.
(10) Almenningen, A.; Halvorsen, S.; Haaland, A. *Acta Chem. Scand.* **1971**, *25*, 1937−1945.
(11) Huffman, J. C.; Streib, W. E. *Chem. Commun.* **1971**, 910−911.
(12) Byram, S. K.; Fawcett, J. K.; Nyburg, S. C.; O'Brien, R. J. *Chem. Commun.* **1970**, 16−17.
(13) Vranka, R. G.; Amma, E. L. *J. Am. Chem. Soc.* **1967**, *89*, 3121.
(14) Frisch, M. J.; G.W.T.; Schlegel, H. B.; Gill, P. M. W.; Johnson, M.A.R. B. G.; Cheeseman, J. R.; Keith, T.; Petersson, J.A.M. G. A.; Raghavachari, K.; Al-Laham, V.G.Z. M. A.; Ortiz, J. V.; Foresman, J. B.; Cioslowski, B.B.S. J.; Nanayakkara, A.; Challacombe, M.; Peng, P.Y.A. C. Y.; Chen, W.; Wong, M. W.; Andres, J. L.; Replogle, R.G. E. S.; Martin, R. L.; Fox, D. J.; Binldey, D.J.D. J. S.; Baker, J.; Stewart, J. P.; Head-Gordon, C.G. M.; Pople, J. A. *Gaussian 94*; Gaussian Inc.: Pittsburgh, PA, 1995.
(15) Møller, C.; Plesset, M. S. *Phys. Rev.* **1934**, *46*, 618.
(16) Krishnan, R.; Pople, J. A. *Int J. Quantum Chem.* **1978**, *14*, 91.
(17) Krishnan, R.; Frisch, M. J.; Pople, J. A. *J. Chem. Phys.* **1980**, *72*, 4244−4245.
(18) Pople, J.A.; Krishnan, J. A.; Schlegel, H. B.; Binkley, J. S. *Int. J. Quantum Chem.* **1978**, *14*, 545.
(19) Scuseria, G. E.; Janssen, C. L.; Schaefer, H. F. *J. Chem. Phys.* **1989**, *90*, 3700.
(20) Cisek, J. *Adv. Chem. Phys.* **1969**, *14*, 35.
(21) Pople, J. A.; Head-Gordon, M.; Raghavachari, K. *J. Chem. Phys.* **1987**, *87*, 5968.
(22) Casida, M. E.; Daul, C.; Goursot, A.; Koester, A.; Pettersson, L.; Proynov, E.; St-Amant, A.; Salahub, D. R.; Duarte, H.; Godbout, N.; Guan, J.; Jamorski, C.; Lebouf, M.; Malkin, V.; Malkina, O.; Sim, F.; Vela, A. deMon-KS module release 3.1.; deMon software, University of Montreal, 1996.
(23) Becke, A. D. *Phys. Rev. A* **1988**, *38*, 3098.
(24) Perdew, J. P. *Phys. Rev. B.* **1986**, *33*, 8822.
(25) Perdew, J. P.; Wang, Y. *Phys. Rev.* **1992**, *45*, 13244.
(26) Godbout, N.; Salahub, D. R.; Andzelm, J.; Wimmer, E. *Can. J. Chem.* **1992**, *70*, 560.
(27) Mayer, I. *Phys. Lett.* **1983**, *97*, 270.
(28) Boys, S. F.; Bernardi, F. *Mol. Phys.* **1970**, *19*, 553.
(29) Atiya, G. A.; Grady, A. S.; Russell, D. K.; Claxton, T. A. *Spectrochim. Acta* **1991**, *47A*, 467−476.
(30) Winters, R. E.; Kiser, R. W. *J. Organomet. Chem.* **1967**, *10*, 7−15.
(31) Bews, J.; Glidewell, R. *J. Mol. Struct.* **1982**, *90*, 151−163.
(32) Tsang, W. Heats of formation of organic free radicals by kinetic methods. In *Energetics of Organic Free Radicals*; Simoes, M., Greenberg, J., Liebman, J. F., Eds.; Blackie Academic & Professional: London 1996; pp 22−58.
(33) Hiraoka, Y.; Someya; Mashita, M. *J. Cryst. Growth* **1994**, *145*, 473−477.
(34) Barker, G. K.; Lappert, M. F.; Pedley, J. B.; Sharp, G. J.; Westwood, N. P. C. *J. Chem. Soc., Dalton Trans.* **1975**, 1765.
(35) Baker, J.; Scheiner, A.; Andzelm, J. *Chem. Phys. Lett.* **1993**, *216*, 38.
(36) Eriksson, L. A.; Malkina, O. L.; Malkin, V. G.; Salahub, D. R. *J. Chem. Phys.* **1994**, *100*, 5066.
(37) Hiraoka, Y. S.; Mashita, M.; Tada, T.; Yoshimura, R. *J. Cryst. Growth* **1993**, *128*, 494−498.
(38) Ogawa, T. *Spectrochim. Acta* **1968**, *24A*, 15−20.
(39) Kvisle, S.; Rytter, E. *Spectrochim. Acta* **1984**, *40A*, 939.